Inorganic Chemistry

Article

pubs.acs.org/IC

Irida-β-ketoimines Derived from Hydrazines To Afford Metallapyrazoles or N−N Bond Cleavage: A Missing Metallacycle Disclosed by a Theoretical and Experimental Study

Itziar Zumeta,[†] Claudio Mendicute-Fierro,[†] Itxaso Bustos,[†] Miguel A. Huertos,[†,‡] Antonio Rodríguez-Diéguez,[§] José M. Seco,[†] Eider San Sebastian,[†] and María A. Garralda*[,†]

[†]Facultad de Química de San Sebastián, Universidad del País Vasco (UPV/EHU), Apdo. 1072, 20080 San Sebastián, Spain

[‡]Ikerbasque, Basque Foundation for Science, 48013 Bilbao, Spain

[§]Facultad de Ciencias, Universidad de Granada, Avda. Fuenteventura s/n, 18071 Granada, Spain

Supporting Information

ABSTRACT: Unprecedented metallapyrazoles [$IrH_2\{Ph_2P(o\text{-}C_6H_4)CNNHC(o\text{-}C_6H_4)PPh_2\}$] (**3**) and [$IrHCl\{Ph_2P(o\text{-}C_6H_4)\text{-}CNNHC(o\text{-}C_6H_4)PPh_2\}$] (**4**) were obtained by the reaction of the irida-β-ketoimine [$IrHCl\{(PPh_2(o\text{-}C_6H_4CO))(PPh_2(o\text{-}C_6H_4CNNH_2))H\}$] (**2**) in MeOH heated at reflux in the presence and absence of KOH, respectively. In solution, iridapyrazole **3** undergoes a dynamic process due to prototropic tautomerism with an experimental barrier for the exchange of $\Delta G^{\ddagger}_{coal}$ = 53.7 kJ mol^{-1}. DFT calculations agreed with an intrapyrazole proton transfer process assisted by two water molecules (ΔG = 63.1 kJ mol^{-1}). An X-ray diffraction study on **4** indicated electron delocalization in the iridapyrazole ring. The reaction of the irida-β-diketone [$IrHCl\{(PPh_2(o\text{-}C_6H_4CO))_2H\}$] (**1**) with H_2NNRR' in aprotic solvents gave irida-β-ketoimines [$IrHCl\{(PPh_2(o\text{-}C_6H_4CO))(PPh_2(o\text{-}C_6H_4CNNRR'))H\}$] (R = R′ = Me (**5**); R = H, R′ = Ph (**8**)), which can undergo N−N bond cleavage to afford the acyl−amide complex [$IrHCl(PPh_2(o\text{-}C_6H_4CO))(PPh_2(o\text{-}C_6H_4C(O)N(CH_3)_2))$-κ*P*,κ*O*] (**6**) or [$IrHCl(PPh_2(o\text{-}C_6H_4CO))(PPh_2(o\text{-}C_6H_4CN)$-κ*P*)$(NH_2NHPh$-κ*NH*$_2)$] (**9**) containing *o*-(diphenylphosphine)benzonitrile and phenylhydrazine, respectively. From a CH_2Cl_2/CH_3OH solution of **9** kept at −18 °C, single crystals of [$IrHCl(PPh_2(o\text{-}C_6H_4CO))(PPh_2(o\text{-}C_6H_4CN)$-κ*P*))$(HN{=}NPh$-κ*NH*)] (**10**) containing *o*-(diphenylphosphine)benzonitrile and phenyldiazene were formed, as shown by X-ray diffraction. The reaction of **1** with methylhydrazine in methanol gave the hydrazine complex [$IrCl(PPh_2(o\text{-}C_6H_4CO))_2(NH_2NH(CH_3)$-κ*NH*$_2)$] (**7**). Single-crystal X-ray diffraction analysis was performed on **6** and **7**.

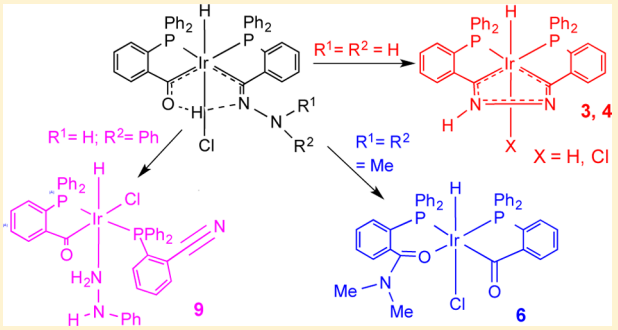

INTRODUCTION

Hydrazines, formed by two bonded nucleophilic nitrogen atoms, possess a wide range of useful properties,[1] including the syntheses of heterocycles[1,2] and cleavage of the N−N bond,[3] that are relevant in organic syntheses. They have also attracted considerable interest as ligands to transition metals because of their importance in biological nitrogen fixation under mild conditions.[4] The formation of hydrazine complexes that then undergo protonation and cleavage of the N−N bond is believed to be involved in one of the last steps of metal-promoted nitrogen reduction.[5] Consequently a large number of transition metal complexes containing hydrazines coordinated as κ^1-monodentate, κ^2-bidentate to a single metal center, or μ-κ^2-bridging ligands have been described.[6,7] Studies on the reactivity of iridium compounds with hydrazines are limited. A few iridium(III) complexes containing κ^1-NH_2NHR or μ-κ^2 coordination have been reported,[8] and iridium(I) complexes promote the N−H activation of 1,2-diphenylhydrazine or 1-aminopiperidine to afford cyclometalated azobenzene derivatives or hydridohydrazido or aminonitrene complexes, respectively.[9] Metalla-β-diketones can be considered as enol tautomers of neutral β-diketones in which the methine group has been substituted by a transition metal organometallic fragment, so they may also be understood as acyl(hydroxycarbene) complexes that are stabilized by an intramolecular hydrogen bond between the acyl and hydroxycarbene moieties (**1** in Chart 1). The reaction of the rhena-β-diketone *cis*-[$Re(CO)_4\{(C(CH_3)O)_2H\}$] with H_2NNHR (R =

Chart 1

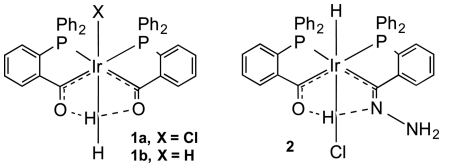

Received: June 29, 2016
Published: September 30, 2016

DOI: 10.1021/acs.inorgchem.6b01550
Inorg. Chem. 2016, 55, 10284−10293

H, Me, Ph) has been reported to lead to N−N bond cleavage and the formation of acetyl−amine complexes *cis*-[Re(CO)$_4$(COCH$_3$)(NH$_2$R)] and acetonitrile, and it was suggested that the reaction could involve intermediates of the rhena-β-ketoimine type.[10] We have recently shown that hydrazine reacts with the irida-β-diketone [IrHCl{(PPh$_2$(*o*-C$_6$H$_4$CO))$_2$H}] (**1a**) to give the ketoimine-type complex [IrHCl{(PPh$_2$(*o*-C$_6$H$_4$CO))(PPh$_2$(*o*-C$_6$H$_4$CNNH$_2$))H}] (**2**)[11] (Chart 1). Complex **2** is similar to other irida-β-ketoimines obtained from ammonia or aliphatic primary amines.[12] The latter easily undergo hydrolysis or deprotonation in protic media at room temperature, which were not observed for **2**. Therefore, we thought it useful to further study the reactivity of **2** and also that of new irida-β-ketoimines derived from substituted hydrazines. Here we report on the formation of unprecedented metallapyrazole complexes and on the cleavage of the N−N bond in substituted hydrazines to afford amides or nitriles under mild reaction conditions or the formation of hydrazine complexes depending on the hydrazine and/or the reaction conditions used.

RESULTS AND DISCUSSION

Formation of Metallapyrazoles. When irida-β-ketoimine **2** is heated at reflux in MeOH in the presence of KOH, nucleophilic attack of the pendant amino group to the hydroxycarbene fragment followed by imination occurs to afford the iridapyrazole [IrH$_2$\{Ph$_2$P(*o*-C$_6$H$_4$)CNNHC(*o*-C$_6$H$_4$)PPh$_2$\}] (**3**), as shown in Scheme 1i. To the best of our knowledge, this is the first reported example of a metallapyrazole. The formation of **3** also involves an exchange of chloride for hydride that may occur by substitution of chloride by methoxide (generated in MeOH/KOH) followed by β-hydrogen transfer to the metal. This sequence may afford the dihydrido species and formaldehyde.[13] Complex **1a** (Chart 1) undergoes such exchange to produce the dihydridoirida-β-diketone [IrH$_2$\{(PPh$_2$(*o*-C$_6$H$_4$CO))$_2$H\}] (**1b**).[14] Attempts to obtain **3** by the reaction of **1b** with hydrazine proved unsuccessful.

Scheme 1. Formation of Hydridoiridapyrazoles 3 and 4: (i) In MeOH/KOH Heated at Reflux; (ii) In MeOH Heated at Reflux

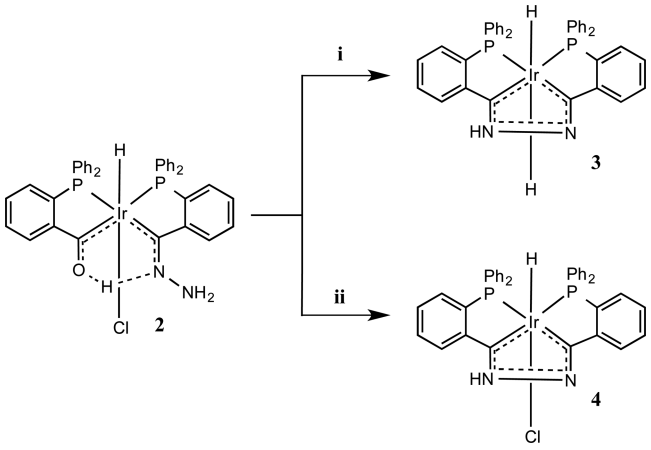

The ESI-MS spectrum supports the formation of [IrH$_2$\{Ph$_2$P(*o*-C$_6$H$_4$)CNNHC(*o*-C$_6$H$_4$)PPh$_2$\}] **3**, showing peaks at m/z = 769.15 and 771.14 due to $[M - H]^+$ and $[M + H]^+$ species, respectively (Figure SI-1 in the Supporting Information). The NMR spectra show that **3** undergoes a dynamic process at room temperature, and thus, the spectra were measured at −60 °C in CDCl$_3$ (Figure SI-2). The low solubility of complex **3** precluded any $^{13}C\{^1H\}$ NMR measurement. The mutually trans hydrido ligands appear equivalent in the ^{1}H NMR spectrum as a triplet at −9.82 ppm (^2J(P,H) = 21.1 Hz) due to two cis phosphorus atoms. A resonance in the low-field region at 13.28 ppm confirms the presence of the NH fragment. In accordance with this, the $^{31}P\{^1H\}$ NMR spectrum shows two singlets at 21.1 and 13.3 ppm due to two nonequivalent phosphorus atoms. With increasing temperature the signals due to the phosphorus atoms broaden and then collapse at 20 °C. The signal due to NH also gets broader and finally collapses as the temperature increases, while the signal due to the hydrido ligands remains unchanged throughout the process (Figure SI-3). These observations suggest a proton transfer process between the nitrogen atoms that would render the phosphorus atoms equivalent. Fluxional behavior in pyrazoles due to prototropic tautomerism is very common.[15] Therefore, we propose the exchange shown in Scheme 2 to be responsible for the observed fluxional behavior of **3**. From the $^{31}P\{^1H\}$ NMR spectra, barrier for this exchange of $\Delta G^{\ddagger}_{coal}$ = 53.7 kJ mol^{-1} can be calculated ($\Delta G^{\ddagger}_{coal}$ = $19.12T_c[10.32 + \log(T_c/k_c)]$, in which $k_c = (\pi/\sqrt{2})\Delta\nu$, $\Delta\nu$ = 729 Hz, and T_c = 293 K).

Scheme 2. Prototropic Tautomerism in Iridapyrazole 3

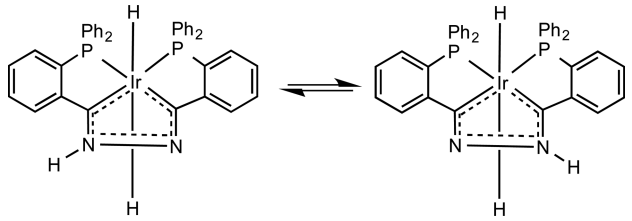

In order to gain some insights into the mechanism by which the prototropism occurs, DFT calculations were carried out. Several proton transfer reaction mechanisms that may explain the tautomerism-derived fluxionality observed experimentally were analyzed. The first type of mechanism studied (Scheme 3a) sits on the assumption that an inter-metallapyrazole proton transfer occurs upon the formation of a dimer involving two N−H···N hydrogen-bonded monomers of **3**. In this line, intermolecular proton transfer processes occurring in multimeric complexes formed by mutually facing pyrazole monomers have been described previously,[15b,15d,15f] in which the kinetic barriers for the proton exchange depend on the nature of the substituents on the pyrazole rings. The second type of mechanism (Scheme 3b−d) involves a proton transfer from the N−H group of the metallapyrazole moiety in **3** in monomer form to the neighboring N atom of the same metallapyrazole moiety. According to the literature,[15d] this intra-pyrazole proton transfer process is usually assisted by either one or two water molecules, since the ability of the latter to behave as a strong H-bond donor/acceptor significantly lowers the free energy barrier of the nonassisted process (Scheme 3b). In the present study, the effect on such a barrier of an explicit interaction of **3** with either one (Scheme 3c) or two water molecules (Scheme 3d) was studied. In any case, the solvent-corrected free energy barriers (ΔG herein) for the different mechanisms proposed were computed and compared (see the Experimental Section).

DOI: 10.1021/acs.inorgchem.6b01550
Inorg. Chem. 2016, 55, 10284−10293

Scheme 3. Proton Transfer Mechanisms in 3: (a) Inter-metallapyrazole Proton Transfer Mechanism upon Formation of a Dimer of 3; (b) Nonassisted Intra-metallapyrazole Proton Transfer Mechanism; (c, d) Intra-metallapyrazole Proton Transfer Mechanisms Assisted by (c) One or (d) Two Water Molecules

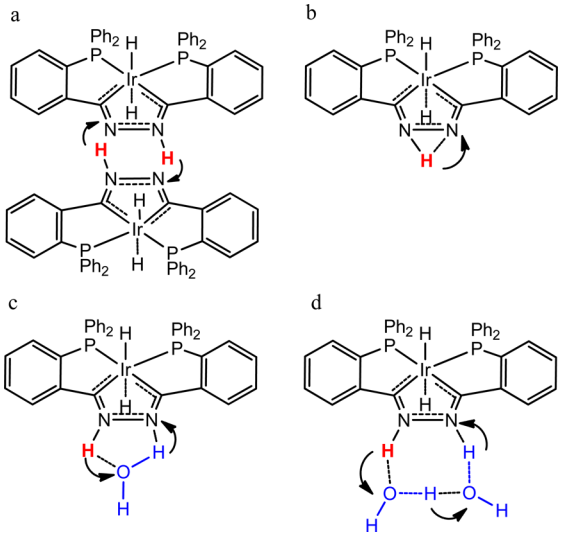

For the inter-metallapyrazole proton transfer mechanism, we propose that two monomers of **3** in a particular tautomeric state form a dimer via two distinct intermolecular N−H···N hydrogen bonds (Scheme 3a). DFT calculations failed to capture a transition state (TS) associated with a concerted proton transfer mechanism. Instead, a stepwise proton transfer mechanism was proved to be plausible. It begins with the formation of a dimer of **3** showing a particular tautomer form, which is followed by two consecutive intermolecular proton transfer steps that yield a dimer with a doubly protonated (NH−NH) partner first and finally a dimer of **3** in the second tautomer form (Figure SI-4). The overall barrier of this mechanism (113.5 kJ mol^{-1}; Table SI-1) was estimated to be much higher than the experimental one ($\Delta G^{\ddagger}_{coal}$ = 53.7 kJ mol^{-1}).

For the intra-metallapyrazole proton transfer mechanism, three alternative pathways were studied. As shown in Figure 1 and Table 1, the intra-metallapyrazole mechanism begins with an initial tautomer of **3** in its monomer form (mT1) and needs to overcome a single barrier to afford the second tautomer form (mT2). In the case of a direct proton transfer mechanism, the barrier to afford the corresponding TS (mTS1) is too high to be overcome at room temperature (ΔG = 242.4 kJ mol^{-1}). As expected, the energy of such a barrier is significantly lowered when the process is water-assisted: 130.4 kJ mol^{-1} (mTS1_1w, one H_2O in Table 1) and 63.1 kJ mol^{-1} (mTS1_2w, two H_2O in Table 1), when one or two water molecules, respectively, are involved in the reaction. The latter mechanism yields energy values in very good agreement with the experimental results ($\Delta G^{\ddagger}_{coal}$ = 53.7 kJ mol^{-1}).

According to our DFT results, the intra-metallapyrazole mechanism involving monomers and assistance by two water molecules may be the mechanism responsible for the fluxionality observed experimentally. The monomeric form of **3** in solution is also supported by diffusion-ordered spectroscopy (DOSY) experiments. For comparison we used the previously reported dihydridoirida-β-diketone **1b** (Chart 1),[14]

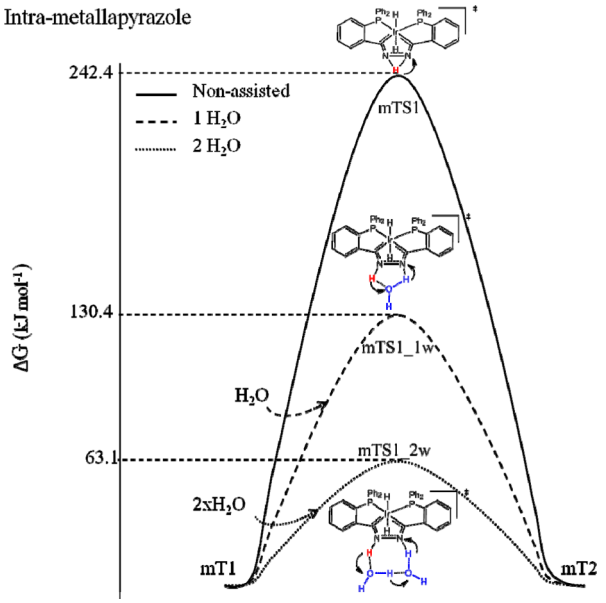

Figure 1. Energy profiles and transition states of the nonassisted intra-metallapyrazole mechanism (mTS1) and the intra-metallapyrazole mechanisms assisted by one water molecule (mTS1_1w) or two water molecules (mTS1_2w).

Table 1. Intra-metallapyrazole Proton Transfer in 3: Relative Free Energies (in kJ mol^{-1}), Considering Solvent Effects (Chloroform), of the Transition States of the Different Intra-metallapyrazole Mechanisms Studied, Calculated at the B3LYP/6-311+G(LANL2DZ)//B3LYP/6-31+G* (LANL2DZ) Level of Theory**

	nonassisted	one H_2O	two H_2O
TS	mTS1	mTS1_1w	mTS1_2w
ΔG (kJ/mol)	242.4	130.4	63.1

since it is a monomer; it shows a hydride resonance at −8.76 ppm and is similar in both size and shape to a monomer of **3**. The hydride signals due to **3** and **1b** were therefore chosen in the 2D ^{1}H DOSY experiment as the references for the corresponding compounds. This experiment, run on a mixture of **3** and **1b** in $CDCl_3$, revealed analogous diffusion coefficients (D) for the two species (0.95×10^{-9} and 1.05×10^{-9} m^2 s^{-1}, respectively; Figure SI-5), suggesting that **3** and **1b** have similar molecular shapes and sizes in solution and therefore the same aggregation state.

Repeated attempts to obtain crystals of dihydridoiridapyrazole **3** proved unsuccessful, though we were fortunate in growing single crystals of the related hydridochloridoiridapyrazole [IrHCl{$Ph_2P(o\text{-}C_6H_4)CNNHC(o\text{-}C_6H_4)PPh_2$}] (**4**) that were suitable for X-ray diffraction, which were obtained from a chloroform solution of **2** kept at 4 °C for several days. Complex **4** could be prepared by heating complex **2** in MeOH at reflux (Scheme 1ii). The extremely low solubility of **4**, which is only slightly soluble in DMF or MeOH, precluded any NMR study. Complex **4** was characterized in methanol solution by ESI-MS, which showed a peak at m/z = 769.15 due to [M − Cl]$^+$ (Figure SI-6).

The ORTEP view of **4** in Figure 2 shows a slightly distorted octahedral coordination sphere around the metal atom with four positions occupied by the PCCP atoms of the new tetradentate ligand and a chloride and a hydride to complete

DOI: 10.1021/acs.inorgchem.6b01550
Inorg. Chem. 2016, 55, 10284−10293

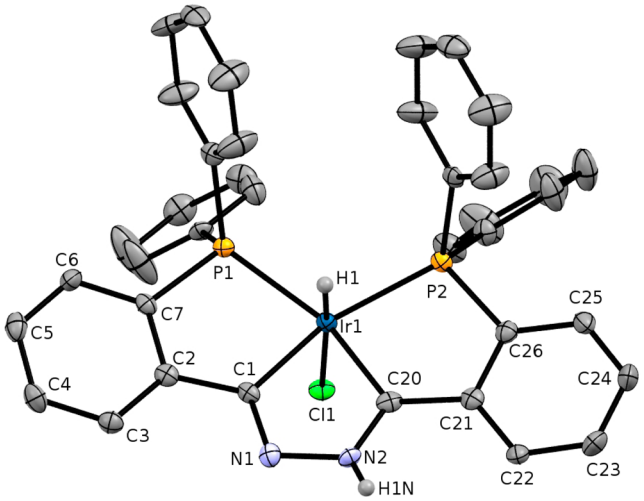

Figure 2. ORTEP plot (50% probability ellipsoids) of complex **4** showing the atomic numbering. All but two of the hydrogen atoms and the labels of some C atoms have been omitted for clarity. Selected bond lengths (Å) and angles (deg): Ir1−P1 2.316(1), Ir1−P2 2.3157(9), Ir1−C1 2.000(3), Ir1−C20 1.974(4), Ir1−H1 1.39(5), Ir1−Cl1 2.4901(9), C1−N1 1.315(5), C20−N2 1.320(4), N1−N2 1.409(4), P1−Ir1−P2 113.20(3), P1−Ir1−C1 84.3(1), P2−Ir1−C20 83.9(1), P1−Ir1−C20 161.3(1), P2−Ir1−C1 160.3(1), C1−Ir1−C20 77.7(1), Ir1−C1−N1 119.6(3), Ir1−C20−N2 113.8(3), C1−N1−N2 108.6(3), C20−N2−N1 120.2(3).

the coordination sphere. The PCCP ligand generates three new chelate rings, all of them five -membered, practically planar, and also coplanar. The best least-squares plane for the Ir1, P1, C7, C2, C1, N1, N2, C20, C21, C26, and P2 atoms shows a maximum deviation of 0.172 Å for the iridium atom, toward the chlorido ligand. Furthermore, the dihedral angles between this plane and the best least-squares-planes formed by atoms C2, C3, C4, C5, C6, and C7 and atoms C21, C22, C23, C24, C25, and C26 are 10.01° and 6.88°, respectively. In the iridapyrazole ring, the maximum deviation of the best least-squares plane of the Ir1, C1, N1, N2, and C20 atoms is 0.010 Å for C1 and C20. The Ir−P and Ir−C distances, in the range of those observed for irida-β-diketones,[17] are equal within the experimental error. The C−N distances are also equal and within the range expected for a pyrazole ring.[18] The N−N distance observed in **4** (1.409(4) Å) is slightly longer than that in organic pyrazoles, but it is meaningfully shorter than that in hydrazines (ca. 1.45 Å) and longer than that found in diazene derivatives (ca. 1.25 Å).[5b,6c,19] These observations indicate a certain degree of electron delocalization in the iridapyrazole ring. The C1−Ir1−C20 angle in the iridacycle (77.7(1)°) is significantly smaller than the C−C−C angle in pyrazoles (ca. 107°), causing the P1−Ir1−P2 angle to be rather large (113.20(3)°). Consequently, the Ir−C−N angles (113.8(3)° and 119.6(3)°) and C−N−N angles (108.6(3)° and 120.3(3)°) in the iridapyrazole are larger than the corresponding values in pyrazoles. The molecules of complex **4** are arranged as dimers because of the formation of intermolecular hydrogen bonds between the NH of the iridapyrazole ring and the chlorido ligand, with the distance N2···Cl1 = 3.271(3) Å and the angle N2−H2N···Cl = 163(4)° (Figure SI-7).

Transition-metal-containing aromatic metallacycles are interesting species that may display unique properties and adopt different structural modes.[20] Metallabenzenes and also several N-, S-, or O-heteroatom-containing systems have been studied, though metallapyrazoles have been elusive and have not been reported before. Complexes **3** and **4** fill a gap in this series and represent the first metallapyrazoles to be reported.

Cleavage of Substituted Hydrazines: Formation of Amides or Nitriles. The formation of iridapyrazole complexes **3** and **4** led us to study the reactivity of irida-β-diketone **1a** with substituted hydrazines that could afford N-substituted metallapyrazoles. Complex **1a** was reacted with methylhydrazine, but unfortunately, this led only to intractable mixtures. Instead, the reaction of compound **1a** with *N,N*-dimethylhydrazine in anhydrous THF gave the corresponding hydridoirida-β-ketoimine [IrHCl{(PPh$_2$(o-C$_6$H$_4$CO))(PPh$_2$(o-C$_6$H$_4$CNN-(CH$_3$)$_2$))H}] (**5**) (Scheme 4i). Complex **5** was unambiguously

Scheme 4[a]

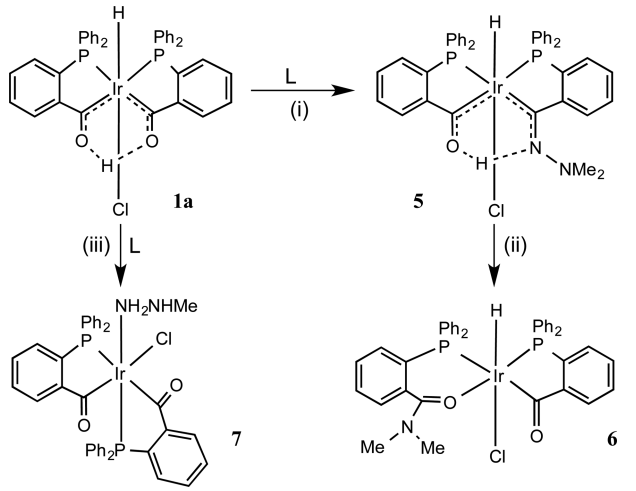

[a]Conditions: (i) L = H_2NNMe_2 in THF; **1a**:L = 1:5. (ii) In MeOH heated at reflux. (iii) L = H_2NNHMe in CH_2Cl_2/MeOH; **1a**:L = 1:1.5.

characterized in solution by NMR spectroscopy and ESI-MS as a metalla-β-ketoimine. In the ^{1}H NMR spectrum, a triplet at −20.70 ppm (^2J(P,H) = 14.1 Hz) corresponds to a hydrido ligand trans to chloride and cis to two phosphorus atoms. The acidic proton appears at 13.95 ppm, and a singlet due to the methyl substituents appears at 2.89 ppm. The ^{31}P{^{1}H} NMR spectrum shows two singlets at 30.8 and 16.3 ppm, indicating two nonequivalent phosphorus atoms in cis relative position, and the ^{13}C{^{1}H} NMR spectrum shows two doublets at 244.6 and 206.7 ppm, with ^2J(P,C) = 107 and 104 Hz, respectively, corresponding to carbon atoms of the keto and imine groups trans to phosphorus.

In methanol heated at reflux, compound **5** is transformed into an acyl−amide complex, [IrHCl(PPh$_2$(o-C$_6$H$_4$CO))-(PPh$_2$(o-C$_6$H$_4$C(O)N(CH$_3$)$_2$))-κ*P*,κ*O*] (**6**) (Scheme 4ii). The reaction occurs with cleavage of the N−N bond and the formation of an amide group bonded to the metal through the oxygen atom, thus affording a six-membered chelate ring. In the ^{1}H NMR spectrum a signal appears as a doublet of doublets at −21.43 ppm (^2J(P,H) = 11.9 and 20.7 Hz), which agrees with a hydride trans to a chloride and cis to two phosphorus atoms. The resonance due to the methyl groups at 4.23 ppm is also observed. The ^{31}P{^{1}H} NMR spectrum shows two resonances at 23.7 and 2.9 ppm, corresponding to two phosphorus atoms that are mutually cis. We assign the signal at 23.7 ppm to the acylphosphine chelate ring, since it forms a five-membered metallacycle, and the resonance at 2.9 ppm to the six-

DOI: 10.1021/acs.inorgchem.6b01550
Inorg. Chem. 2016, 55, 10284−10293

membered amidophosphine chelate ring.[21] The $^{13}C\{^{1}H\}$ NMR spectrum displays a doublet at 237.6 ppm ($^{2}J(P,C)$ = 110 Hz) due to an acyl carbon trans to a phosphorus atom and a signal at 160.9 ppm that can be assigned to the carbon atom of the amide.

X-ray diffraction analysis of crystals of **6** confirmed the structure shown in Scheme 4 with O-coordination of the newly formed amide group. Figure 3 shows an ORTEP view of **6** with

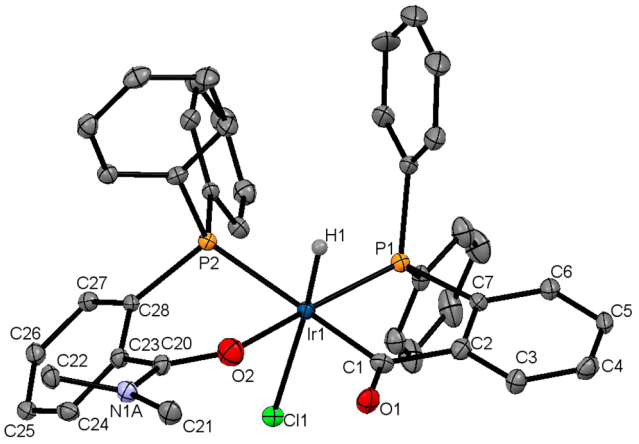

Figure 3. ORTEP plot (50% probability ellipsoids) of complex **6** showing the atomic numbering. All but one of the hydrogen atoms and the labels of some C atoms have been omitted for clarity. Selected bond lengths (Å) and angles (deg): Ir1−P1 2.232(1), Ir1−P2 2.339(1), Ir1−C1 2.040(5), Ir1−O2 2.089(4), Ir1−Cl1 2.498(1), Ir1−H1 1.40(4), C1−O1 1.232(6), C20−O2 1.314(6), C20−N1 1.351(6), P1−Ir1−C1 84.9(1), P2−Ir1−O2 83.3(1), P2−Ir1−C1 165.2(1), P1−Ir1−O2 168.4(1), C23−C20−O2 122.1(4), C23−C20−N1 118.3(4).

the atomic numbering scheme. The distances and angles around the iridium atom are as expected, and the Ir−P distances reflect the trans influence (larger for acyl than for oxygen). The five-membered chelate ring adopts a planar conformation, with C1 showing the maximum deviation of 0.013 Å. The six-membered chelate ring of the amidophosphine ligand adopts a slightly twisted boat conformation.

On account of the nucleophilicity shown by the terminal N atom of coordinated hydrazine-type compounds used as ligands,[4a,22] we believe that the most likely mechanism for the formation of **6** involves nucleophilic attack of the terminal dimethylated N atom to the hydroxycarbene fragment in **5**, similar to that proposed for the formation of iridapyrazoles. In the present case, the imination reaction is unavailable and the cleavage of the N−N bond appears more likely, thus leading to the formation of an amide that can coordinate through the oxygen atom and a C═NH imine fragment whose alcoholysis would give complex **6**. Recently, the transition-metal-catalyzed reaction of amines, including tertiary amines, with aldehydes to afford amides has been a subject of interest.[23] The formation of complex **6** shows the ability of N,N-disubstituted hydrazines to perform this reaction under mild reaction conditions.

Attempts to obtain complexes such as **6** by the reaction of **1a** with methylhydrazines in methanol proved unsuccessful. Instead, the reaction of **1a** with methylhydrazine in methanol led to the hydrazine complex $[IrCl(PPh_2(o\text{-}C_6H_4CO))_2(NH_2NH(CH_3)\text{-}\kappa NH_2)]$ (**7**) (Scheme 4iii). *N,N*-Dimethylhydrazine afforded a similar compound, though unpure. These results show that the formation of an irida-β-ketoimine intermediate is a requirement for the N−N bond cleavage to occur. The ^{1}H NMR spectrum of **7** shows the expected resonances due to the coordinated hydrazine. The $^{31}P\{^{1}H\}$ NMR spectrum contains a signal at 20.7 ppm and a second resonance at 12.7 ppm due to the two nonequivalent phosphorus atoms with a cis disposition, and the $^{13}C\{^{1}H\}$ NMR spectrum shows two different acyl groups, a doublet at 232.6 ppm ($^{2}J(P,C)$ = 108 Hz) that corresponds to an acyl group trans to a phosphorus atom and a doublet at 208.7 ppm ($^{2}J(P,C)$ = 8 Hz) that is due to an acyl group cis to a phosphorus atom.

An X-ray diffraction study on complex **7** confirmed the structure shown in Scheme 4. Figure 4 shows an ORTEP view

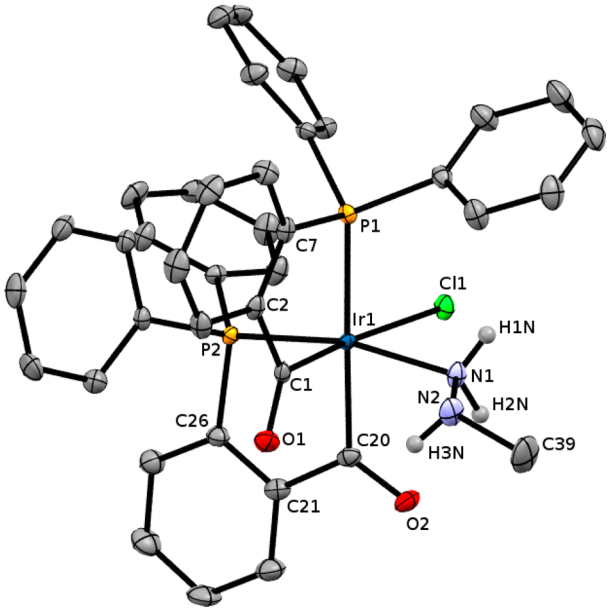

Figure 4. ORTEP plot (50% probability ellipsoids) of complex **7** showing the atomic numbering. All but three of the hydrogen atoms, the labels of some C atoms, and the solvent molecule have been omitted for clarity. Selected bond lengths (Å) and angles (deg): Ir1−P1 2.3569(7), Ir1−P2 2.2760(7), Ir1−Cl1 2.4900(8), Ir1−N1 2.150(2), Ir1−C1 2.015(2), Ir1−C20 2.058(2), N1−N2 1.451(3), P1−Ir1−C20 174.36(7), P2−Ir1−N1 167.08(6), Cl1−Ir1−C1 171.63(7), P1−Ir1−C1 84.38(7), P2−Ir1−C20 83.76(7), N1−N2−C39 110.6(2).

with the atomic numbering scheme. The crystal consists of neutral $[C_{39}H_{34}ClIrN_2O_2P_2]$ molecules and methanol solvent molecules bonded by hydrogen bonds. In the slightly distorted octahedral structure, the methylhydrazine is coordinated to iridium through the less encumbered NH_2 moiety, as expected,[6] and the N−N distance (1.451(3) Å) agrees with the length of a single bond. The chelate rings adopt a planar conformation, and in both of them the maximum deviation from the corresponding Ir−P−C−C−C metallacycle plane is observed for the acyl carbon atom (0.057 Å for C1 and 0.053 Å for C20). The intermolecular hydrogen bond between an acyl group and methanol can be deemed to have moderate strength[24] (O2···O3 = 2.798(3) Å, O2···H−O3 = 173(4)°).

When **1a** is reacted with phenylhydrazine (**1a**:H_2NNHPh = 1:3) in refluxing dichloromethane, the formation of the hydridoirida-β-ketoimine $[IrHCl\{(PPh_2(o\text{-}C_6H_4CO))(PPh_2(o\text{-}C_6H_4CNNHPh))H\}]$ (**8**) is observed (Scheme 5i). Complex **8** was identified by NMR spectroscopy,[25] although it could not be

DOI: 10.1021/acs.inorgchem.6b01550
Inorg. Chem. 2016, 55, 10284−10293

Scheme 5[a]

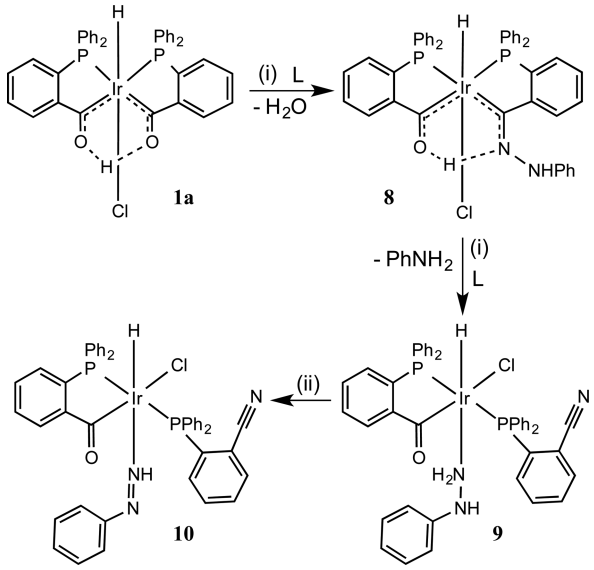

[a](i) L = H_2NNHPh in CH_2Cl_2 heated at reflux; **1a**:L = 1:3. (ii) In CH_2Cl_2/CH_3OH at −18 °C.

isolated pure because it is transformed into complex **9** prior to the complete transformation of **1a** into **8** (Figure SI-8).

The ^1H NMR spectrum of compound **9** shows a triplet at −17.70 ppm ($^2J(P,H)$ = 14.2 Hz) due to a hydrido ligand trans to an electronegative atom and cis to two phosphorus atoms, along with three resonances at 3.47, 3.85, and 5.56 ppm that can be attributed to the coordinated hydrazine. The $^{31}P\{^1H\}$ NMR spectrum of **9** displays two doublets at 33.9 and 25.0 ppm ($^2J(P,P)$ = 362 Hz) corresponding to two phosphorus atoms that are mutually trans. In the low-field region of the $^{13}C\{^1H\}$ NMR spectrum, only a singlet due to the acyl group of an acylphosphine chelate can be observed at 213.9 ppm. A singlet at 118.1 ppm can be attributed to the nitrile shown in Scheme 5, whose presence is also supported by the signal at 2221 cm^{-1} observed in the IR spectrum. The formation of the *o*-(diphenylphosphine)benzonitrile ligand present in **9** can be explained by opening of the hydrogen bond in the ketoimine fragment followed by rearrangement with N−N bond cleavage and release of aniline, as in the previously reported reaction of rhena-*β*-diketones with monosubstituted hydrazines.[10] The formation of **9** also requires isomerization, which is easy upon cleavage of the hydrogen bond in **8**,[12] and coordination of phenylhydrazine. We were unable to obtain single crystals of **9** to perform an X-ray diffraction study. Instead, from a CH_2Cl_2/CH_3OH solution of **9** kept at −18 °C a few X-ray-quality single crystals of [IrHCl(PPh_2(*o*-C_6H_4CO))(PPh_2(*o*-C_6H_4CN)-*κP*))(HN═NPh-*κNH*)] (**10**) containing *o*-(diphenylphosphine)benzonitrile and phenyldiazene moieties were formed, and the structure of **10** supports the presence of the *o*-(diphenylphosphine)benzonitrile and phenylhydrazine in **9**. Figure 5 shows an ORTEP view of **10** with the atomic numbering scheme.

The geometry around the metal in **10** is a distorted octahedron, with two mutually trans phosphorus atoms, one belonging to an acylphosphine chelate and the other to a monodentate-*κP* *o*-(diphenylphosphine)benzonitrile, a hydrido and a phenyldiazene that are mutually trans, and a chloride. The C20−N3 bond length (1.156(8) Å) and the C21−C20−N3 angle (177.3(6)°) confirm the formation of nitrile. For the diazene group, the angles involving the nitrogen atoms (Ir1−N1−N2 = 127.8(3)° and N1−N2−C39 = 117.9(5)°) correspond to sp^2 hybridization, and the N−N distance (1.250(5) Å) is that of a double bond.

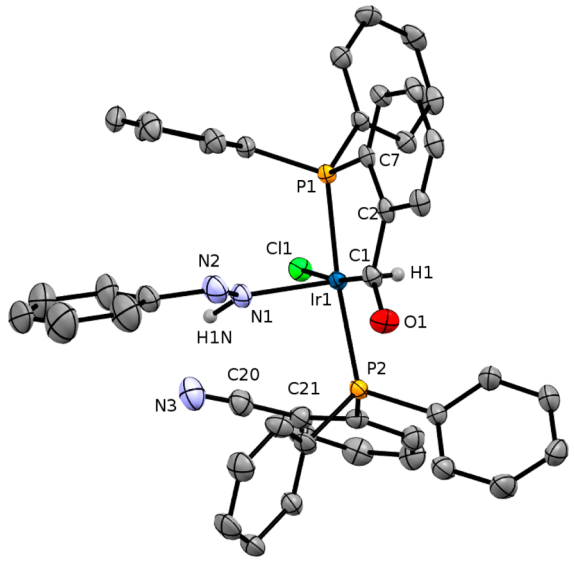

Figure 5. ORTEP plot (50% probability ellipsoids) of complex **10** showing the atomic numbering. All but two of the hydrogen atoms and the labels of some C atoms have been omitted for clarity. Selected bond lengths (Å) and angles (deg): Ir1−P1 2.2713(9), Ir1−P2 2.3428(9), Ir1−Cl1 2.474(1), Ir1−N1 2.120(4), Ir1−C1 1.999(5), Ir1−H1 1.37(7), N1−N2 1.250(5), C20−N3 1.156(8), P1−Ir1−P2 174.65(4), Cl1−Ir1−C1 171.6(1), P1−Ir1−C1 85.7(1), Ir1−N1−N2 127.8(3), N1−N2−C39 117.9(5), N3−C20−C21 177.3(6).

Because arylhydrazine metal complexes can be easily oxidized to aryldiazene derivatives, even at low temperatures,[8c,26] we believe that **9** is a precursor of **10** as shown in Scheme 5ii. We conclude that **9** also contains a P-coordinated *o*-(diphenylphosphine)benzonitrile ligand, formed by cleavage of the N−N bond in irida-*β*-ketoimine **8**, and a coordinated phenylhydrazine, as shown by the NMR and IR spectra.

CONCLUSIONS

The first examples of metallapyrazole compounds are reported. N^1-Unsubstituted iridapyrazoles can be obtained from an irida-*β*-ketoimine derived from hydrazine. According to DFT calculations, the tautomerism-derived fluxionality observed experimentally is due to an intra-metallapyrazole proton transfer mechanism assisted by two water molecules. Irida-*β*-ketoimines derived from N-substituted hydrazines are useful and required intermediates to promote the cleavage of the N−N bond. *N,N*-Dimethylhydrazine allows the formation of a O-coordinated dimethylamide complex under mild conditions, while phenylhydrazine affords a P-coordinated *o*-(diphenylphosphine)benzonitrile. Further studies of metallapyrazoles and related derivatives are presently underway in our laboratory.

EXPERIMENTAL SECTION

General Procedures. The preparation of the metal complexes was carried out at room temperature under nitrogen by standard Schlenk techniques. The complexes [IrHCl{(PPh_2(*o*-C_6H_4CO))$_2$H}] (**1a**)[17] and [IrHCl{(PPh_2(*o*-C_6H_4CO))(PPh_2(*o*-$C_6H_4CNNH_2$))H}] (**2**)[11] were prepared as previously reported. All other chemicals were

DOI: 10.1021/acs.inorgchem.6b01550
Inorg. Chem. 2016, 55, 10284−10293

purchased from commercial sources and used without further purification. Microanalyses were carried out with a Leco CHNS-932 microanalyzer. IR spectra were recorded with a Nicolet FTIR 510 spectrophotometer in the range of 4000−400 cm^{-1} using KBr pellets. ^1H and $^{13}C\{^1H\}$ (TMS internal standard) and $^{31}P\{^1H\}$ (H_3PO_4 external standard) NMR spectra were recorded with a Bruker Avance DPX 300 or Bruker Avance 500 spectrometer. ESI-MS spectra were recorded on a Bruker MicrOTOF-Q Instrument (Universidad de Zaragoza). All of the measurements for the DOSY experiments were performed on a Bruker Avance III 500 with a BBI gradient probe head for 5 mm NMR tubes. The standard Bruker pulse program ledbpgp2s was applied to obtain the spectra at 298 K. For each free induction decay, 512 transients were collected with 2 s relaxation delay, and 64k data points in the F2 dimension (60 ppm) and 24 data points (gradient strengths) in the F1 dimension were collected for all experiments. The diffusion time (Δ) and the gradient length (δ) were set to 100 and 2 ms, respectively, while the recovery delay after gradient pulses was 200 μs. The data were processed using Bruker Topspin version 3.2.

Synthesis and Characterization. *Preparation of [IrH_2{Ph_2P(o-C_6H_4)CNNHC(o-C_6H_4)PPh_2}] (**3**).* To a methanol (3 mL) suspension of **2** (30 mg, 0.036 mmol) was added KOH (2.6 mg, 0.036 mmol). The obtained suspension was heated to 65 °C for 3 h. After cooling, the yellow solid was decanted, washed with methanol, and vacuum-dried. Yield: 7.7 mg, 27%. IR (cm^{-1}): 1764 (m), ν(IrH). ESI-MS (m/z): calcd for $[M - H]^+$ 769.15, observed 769.15; calcd for $[M + H]^+$ 771.14, observed 771.14. Anal. Calcd for $C_{38}H_{31}IrN_2P_2{\cdot}CH_3OH$: C, 58.42; H, 4.40; N, 3.49. Found: C, 58.01; H, 3.85; N, 3.73. ^1H NMR ($CDCl_3$, 213 K): δ 13.28 (s, 1H, NH); −9.82 (t, 1H, ^2J(P,H) = 21.1 Hz, IrH); 9.00−7.00 (m, 28H, aromatic). $^{31}P\{^1H\}$ NMR ($CDCl_3$, 213 K): δ 21.1 (s); 17.5 (s).

*Preparation of [IrHCl{Ph_2P(o-C_6H_4)CNNHC(o-C_6H_4)PPh_2}] (**4**).* A suspension of **2** (20 mg, 0.024 mmol) in methanol (3 mL) was heated to 65 °C for 3 h. After cooling, the orange solid was decanted and vacuum-dried. Yield: 12 mg, 65%. IR (cm^{-1}): 2189 (s), ν(IrH). ESI-MS (m/z): calcd for $[M - Cl]^+$ 769.15, observed 769.15. Anal. Calcd for $C_{38}H_{30}ClIrN_2P_2$: C, 56.75; H, 3.76; N, 3.48. Found: C, 56.73; H, 3.89; N, 3.86.

*Preparation of [IrHCl{(PPh_2(o-C_6H_4CO))(PPh_2(o-$C_6H_4CNN(CH_3)_2$))-H}] (**5**).* To a THF (3 mL) solution of **1a** (30 mg, 0.037 mmol) was added *N*,*N*-dimethylhydrazine (14.1 μL, 0.186 mmol). Stirring for 24 h and evaporation of the solvent gave a yellow solid that was washed with diethyl ether and vacuum-dried. Yield: 22.4 mg, 71%. IR (cm^{-1}): 2199 (m), ν(IrH); 1598 (s), ν(C═O). ESI-MS (m/z): calcd for $[M - Cl]^+$ 815.19, observed 815.19. Anal. Calcd for $C_{40}H_{36}ClIrN_2OP_2$: C, 56.50; H, 4.27; N, 3.29. Found: C, 56.51; H, 4.73; N, 3.31. ^1H NMR ($CDCl_3$): δ 13.95 (s, 1H, N···H···O); 8.99 (m, 1H, aromatic); 7.99 (m, 1H, aromatic); 7.50−7.00 (m, 26H, aromatic); 2.89 (s, 6H, CH_3); −20.70 (t, 1H, ^2J(P,H) = 14.1 Hz, IrH). $^{31}P\{^1H\}$ NMR ($CDCl_3$): δ 30.8 (s); 16.2 (s). $^{13}C\{^1H\}$ NMR ($CDCl_3$): δ 244.6 (d, ^2J(P,C) = 107 Hz, IrC═O); 206.7 (d, ^2J(P,C) = 104 Hz, IrC═N); 165.0−120.0 (aromatic); 47.0 (s, CH_3).

*Preparation of [IrHCl(PPh_2(o-C_6H_4CO))(PPh_2(o-$C_6H_4C(O)N(CH_3)_2$)-κP,κO)] (**6**).* A methanol (3 mL) suspension of **5** (50 mg, 0.059 mmol) was heated at reflux for 10 min, whereupon a yellow solution was obtained. Evaporation of the solvent gave a yellow solid that was recrystallized from chloroform/hexane. Yield: 34.7 mg, 69%. IR (cm^{-1}): 2183 (m), ν(IrH); 1632 (s), 1597 (s), ν(C═O). Anal. Calcd for $C_{40}H_{35}ClIrNO_2P_2{\cdot}CHCl_3$: C, 50.73; H, 3.74; N, 1.44. Found: C, 50.04; H, 3.97; N, 1.29. ^1H NMR ($CDCl_3$): δ 9.70 (m, 1H, aromatic); 8.50−6.50 (m, 27H, aromatic); 4.23 (s, 6H, CH_3); −21.41 (dd, 1H, ^2J(P,H) = 11.9 Hz; ^2J(P,H) = 20.7 Hz, IrH). $^{31}P\{^1H\}$ NMR ($CDCl_3$): δ 23.7 (s); 2.9 (s). $^{13}C\{^1H\}$ NMR ($CDCl_3$): δ 237.6 (d, ^2J(P,C) = 110 Hz, IrC═O); 160.9 (s, NC═O); 160.0−120.0 (aromatic); 54.9 (s, CH_3).

*Preparation of [IrCl(PPh_2(o-C_6H_4CO))$_2$($NH_2NH(CH_3)$-κNH_2)] (**7**).* To a dichloromethane/methanol (1:1) solution (3 mL) of **1a** (30 mg, 0.037 mmol) was added methylhydrazine (0.056 mmol). The solution was stirred for 24 h. Evaporation of the solvents gave a yellow solid that was washed with diethyl ether and vacuum-dried. Yield: 18.3 mg, 58%. IR (cm^{-1}): 3317 (w), 3280 (w), ν(N−H); 1619 (s), ν(C═O). Anal. Calcd for $C_{39}H_{34}ClIrN_2O_2P_2{\cdot}CH_3OH$: C, 54.33; H, 4.33; N, 3.17. Found: C, 54.33; H, 4.22; N, 3.82. ^1H NMR ($CDCl_3$): δ 8.50−6.50 (m, 28H, aromatic); 6.13 (br, 1H, NH_2); 4.19 (br, 1H, NH_2); 3.29 (br, 1H, NH); 2.25 (s, 3H, CH_3). $^{31}P\{^1H\}$ NMR ($CDCl_3$): δ 20.7 (d, ^2J(P,P) = 5 Hz); 12.7 (d). $^{13}C\{^1H\}$ NMR ($CDCl_3$): δ 232.6 (d, ^2J(P,C) = 108 Hz, IrC═O); 208.7 (d, ^2J(P,C) = 8 Hz, IrC═O); 160.0−120.0 (aromatic); 42.5 (d, ^4J(P,C) = 3 Hz, CH_3).

*Preparation of [IrHCl(PPh_2(o-C_6H_4CO)-κP)(PPh_2(o-C_6H_4CN))-(NH_2NHPh-κNH_2)] (**9**).* To a dichloromethane (3 mL) solution of **1a** (20 mg, 0.025 mmol) was added phenylhydrazine (7.3 μL, 0.074 mmol). The suspension was refluxed for 18 h. Evaporation of the solvent gave a yellow solid that was recrystallized from dichloromethane/hexane. Yield: 13.9 mg, 61%. IR (cm^{-1}): 3282 (br), ν(N−H); 2221 (m), ν(C≡N); 2169 (m), ν(IrH); 1600 (m), ν(C═O). Anal. Calcd for $C_{44}H_{37}ClIrN_3OP_2$: C, 57.86; H, 4.08; N, 4.60. Found: C, 57.57; H, 4.50; N, 4.33. ^1H NMR ($CDCl_3$): δ 8.50−6.50 (m, 33H, aromatic); 5.56 (s, 1H, NH); 3.85 (s, 1H, NH_2); 3.47 (s, 1H, NH_2); −17.70 (t, 1H, ^2J(P,H) = 14.2 Hz, IrH). $^{31}P\{^1H\}$ NMR ($CDCl_3$): δ 33.9 (d, ^2J(P,P) = 362 Hz); 25.0 (d). $^{13}C\{^1H\}$ NMR ($CDCl_3$): δ 213.9 (s, IrC═O); 165.0−120.0 (aromatic); 118.1 (s, C≡N).

X-ray Structure Analysis. Crystals of compound **4** suitable for X-ray experiments were obtained from a chloroform solution of **2** kept at 4 °C. For compounds **6**, **7**, and **10**, X-ray-quality crystals were obtained by slow vapor diffusion of diethyl ether onto chloroform (**6**), dichloromethane/methanol (**7**), or methanol (**10**) solutions at −20 °C. In all cases a crystal was coated with epoxy resin and mounted on a Bruker D8 Venture diffractometer equipped with a photon detector and graphite-monochromatized Mo Kα radiation (λ = 0.71073 Å) operating at 50 kV and a temperature of 100 K. The cell parameters were determined and refined by least-squares fitting of all reflections collected. The first 100 frames were recollected at the end of the data collection to monitor the crystal decay, and no appreciable decay was observed. In four cases, an empirical absorption correction was applied. The data reduction was performed with the APEX2[27] software, and the data were corrected for absorption using SADABS.[28] Crystal structures were solved by direct methods using the SIR97 program[29] and refined by full-matrix least-squares on F^2 including all reflections using anisotropic displacement parameters by means of the WINGX crystallographic package.[30] In all cases, the hydrogen atoms were included at their calculated positions as determined by molecular geometry and refined riding on the corresponding bonded atoms, except for the hydrides bonded to the Ir atom and the H atoms bonded to nitrogen atoms, which were located from the Fourier map and included. Several crystals of compounds **4** and **6** were measured, and the structures were solved from the best data that we were able to collect. Attempts to solve disorder problems with chloroform solvent molecules in compounds **4** and **6** failed. Instead, a new set of $F^2(hkl)$ values with the contribution from solvent molecules withdrawn was obtained by the SQUEEZE procedure implemented in PLATON-94.[31] Final $R(F)$, $wR(F^2)$, and goodness-of-fit agreement factors and details regarding the data collection and analysis can be found in Table SI-2.

Computational Studies. Quantum-chemical calculations were carried out with the Gaussian 09 program suite.[32] Full geometry optimization of each species was performed in the gas phase using the B3LYP hybrid density functional[33] with the 6-31+G* basis set for nonmetal atoms together with the LANL2DZ basis set[34] for the metal. Energy values were then refined by single-point calculations on the B3LYP/LANL2DZ geometries at the B3LYP/6-311+G**+LANL2DZ level of theory, and solvent (chloroform) contributions to the free energy were considered by means of polarizable continuum model (PCM) calculations.[35] The nature of the stationary points was verified by analytical computations of harmonic vibrational frequencies. A pressure of 1 atm and a temperature of 298.15 K were assumed in the calculations. Free enthalpies were derived from the sum of electronic and thermal enthalpies (ε_o and H_{corr} in Gaussian), whereas free energies were computed as the sum of electronic and thermal free energies (ε_o and G_{corr} in Gaussian).

DOI: 10.1021/acs.inorgchem.6b01550
Inorg. Chem. 2016, 55, 10284−10293

■ ASSOCIATED CONTENT

Supporting Information

The Supporting Information is available free of charge on the ACS Publications website at DOI: 10.1021/acs.inorgchem.6b01550.

Crystallographic data for **4**, **6**, **7**, and **10** (CIF)

ESI-MS and NMR spectra, energy profile of the intermetallapyrazole proton transfer mechanism for **3**, and geometries of structures described in the article (PDF)

■ AUTHOR INFORMATION

Corresponding Author

*E-mail: mariaangeles.garralda@ehu.es.

Notes

The authors declare no competing financial interest.

■ ACKNOWLEDGMENTS

Partial financial support by Ministerio de Economía y Competitividad (CTQ2015-65268-C2-1-P and CTQ2015-65268-C2-2-P), Gobierno Vasco (S-PE13UN023), and Universidad del País Vasco (UPV/EHU) (GIU 13/06) is gratefully acknowledged. I.Z. is grateful to Gobierno Vasco for a scholarship. Technical and human support provided by IZO-SGI, SGIker (UPV/EHU, MICINN, GV/EJ, ERDF, and ESF) is gratefully acknowledged.

■ REFERENCES

(1) Schmidt, E. W. *Hydrazine and Its Derivatives: Preparation, Properties, Applications*, 2nd ed.; Wiley-VCH: Weinheim, Germany, 2001.

(2) (a) Katritzky, A. R. *Handbook of Heterocyclic Chemistry*; Pergamon Press: New York, 1985; p 416. (b) Engelhardt, U. Nonalternating Inorganic Heterocycles Containing Hydrazine as Building Block. *Coord. Chem. Rev.* **2002**, *235*, 53−91. (c) Heller, S. T.; Natarajan, S. R. 1,3-Diketones from Acid Chlorides and Ketones: A Rapid and General One-Pot Synthesis of Pyrazoles. *Org. Lett.* **2006**, *8*, 2675−2678. (d) Manzur, C.; Fuentealba, M.; Hamon, J. R.; Carrillo, D. Cationic Organoiron Mixed-sandwich Hydrazine Complexes: Reactivity Toward Aldehydes, Ketones, β-Diketones and Dioxomolybdenum Complexes. *Coord. Chem. Rev.* **2010**, *254*, 765−780. (e) Willy, B.; Muller, T. J. J. Rapid One-Pot, Four-Step Synthesis of Highly Fluorescent 1,3,4,5-Tetrasubstituted Pyrazoles. *Org. Lett.* **2011**, *13*, 2082−2085. (f) Fustero, S.; Sánchez-Roselló, M.; Barrio, P.; Simón-Fuentes, A. From 2000 to Mid-2010: A Fruitful Decade for the Synthesis of Pyrazoles. *Chem. Rev.* **2011**, *111*, 6984−7034. (g) Dissanayake, A. A.; Odom, A. L. Single-step synthesis of pyrazoles using titanium catalysis. *Chem. Commun.* **2012**, *48*, 440−442.

(3) (a) Gilchrist, T. L. In *Comprehensive Organic Synthesis*; Trost, B. M., Fleming, I., Eds.; Pergamon Press: Oxford, U.K., 1991; Vol. *8*, pp 388−389. (b) Tang, Q.; Zhang, C.; Luo, M. A New Method for N−N Bond Cleavage of N,N-Disubstituted Hydrazines to Secondary Amines and Direct Ortho Amination of Naphthol and Its Analogues. *J. Am. Chem. Soc.* **2008**, *130*, 5840−5841. (c) Martínez, S.; Trepat, E.; Moreno-Mañas, M.; Sebastián, R. M.; Vallribera, A.; Mata, I.; Molins, E. Nitrogen-Nitrogen Bond Cleavage Catalyzed by Ruthenium Complexes. *ARKIVOC* **2007**, *2007* (iv), 170−181. (d) Xu, L.; Wang, Y. C.; Ma, W.; Zhang, W. X.; Xi, Z. Mechanistic Insights into N-N Bond Cleavage in Catalytic Guanylation Reactions between 1,2 Diarylhydrazines and Carbodiimides. *J. Org. Chem.* **2014**, *79*, 12004−12009. (e) Zhao, D.; Shi, Z.; Glorius, F. Indole Synthesis by Rhodium(III)-Catalyzed Hydrazine-Directed C-H Activation: Redox-Neutral and Traceless by N-N Bond Cleavage. *Angew. Chem., Int. Ed.* **2013**, *52*, 12426−12429. (f) Chen, W. J.; Lin, Z. Rhodium(III)-Catalyzed Hydrazine-Directed C−H Activation for Indole Synthesis: Mechanism and Role of Internal Oxidant Probed by DFT Studies. *Organometallics* **2015**, *34*, 309−318.

(4) (a) Hidai, M.; Mizobe, Y. Recent Advances in the Chemistry of Dinitrogen Complexes. *Chem. Rev.* **1995**, *95*, 1115−1133. (b) Burgess, B. K.; Lowe, D. J. Mechanism of Molybdenum Nitrogenase. *Chem. Rev.* **1996**, *96*, 2983−3012. (c) Sellmann, D.; Sutter, J. In Quest of Competitive Catalysts for Nitrogenases and Other Metal Sulfur Enzymes. *Acc. Chem. Res.* **1997**, *30*, 460−469. (d) Fryzuk, M. D.; Johnson, S. A. The Continuing Story of Dinitrogen Activation. *Coord. Chem. Rev.* **2000**, *200−202*, 379−409. (e) Malinak, S. M.; Coucouvanis, D. The Chemistry of Synthetic Fe-Mo-S clusters and their relevance to the Structure and Function of the Fe-Mo-S Center in Nitrogenase. *Prog. Inorg. Chem.* **2001**, *49*, 599−662. (f) MacKay, B. A.; Fryzuk, M. D. Dinitrogen Coordination Chemistry: On the Biomimetic Borderlands. *Chem. Rev.* **2004**, *104*, 385−402.

(5) (a) Hazari, N. Homogeneous iron complexes for the conversion of dinitrogen into ammonia and hydrazine. *Chem. Soc. Rev.* **2010**, *39*, 4044−4056. (b) Crossland, J. L.; Tyler, D. R. Iron−Dinitrogen Coordination Chemistry: Dinitrogen Activation and Reactivity. *Coord. Chem. Rev.* **2010**, *254*, 1883−1894. (c) Umehara, K.; Kuwata, S.; Ikariya, T. N−N Bond Cleavage of Hydrazines with a Multiproton-Responsive Pincer-Type Iron Complex. *J. Am. Chem. Soc.* **2013**, *135*, 6754−6757. (d) Keane, A. J.; Zavalij, P. Y.; Sita, L. R. N−N Bond Cleavage of Mid-Valent Ta(IV) Hydrazido and Hydrazidium Complexes Relevant to the Schrock Cycle for Dinitrogen Fixation. *J. Am. Chem. Soc.* **2013**, *135*, 9580−9583. (e) Gogoi, U.; Guha, A. K.; Phukan, A. K. Tracing the Route to Ammonia: A Theoretical Study on the Possible Pathways for Dinitrogen Reduction with Tripodal Iron Complexes. *Chem. - Eur. J.* **2013**, *19*, 11077−11089. (f) Chang, Y. H.; Chan, P. M.; Tsai, Y. F.; Lee, G. H.; Hsu, H. F. Catalytic Reduction of Hydrazine to Ammonia by a Mononuclear Iron(II) Complex on a Tris(thiolato)phosphine Platform. *Inorg. Chem.* **2014**, *53*, 664−666. (g) Milsmann, C.; Semproni, S. P.; Chirik, P. J. N−N Bond Cleavage of 1,2-Diarylhydrazines and N−H Bond Formation via H-Atom Transfer in Vanadium Complexes Supported by a Redox-Active Ligand. *J. Am. Chem. Soc.* **2014**, *136*, 12099−12107. (h) Rittle, J.; Peters, J. C. An Fe-N_2 Complex That Generates Hydrazine and Ammonia via Fe=NNH_2: Demonstrating a Hybrid Distal-to-Alternating Pathway for N_2 Reduction. *J. Am. Chem. Soc.* **2016**, *138*, 4243−4248.

(6) (a) Kisch, H.; Holzmeier, P. Organometallic Chemistry of the N=N Group. *Adv. Organomet. Chem.* **1992**, *34*, 67−109. (b) Sutton, D. Organometallic Diazo Compounds. *Chem. Rev.* **1993**, *93*, 995−1022. (c) Heaton, B. T.; Jacob, C.; Page, P. Transition Metal Complexes Containing Hydrazine and Substituted Hydrazines. *Coord. Chem. Rev.* **1996**, *154*, 193−229.

(7) (a) Albertin, G.; Antoniutti, S.; Bacchi, A.; Bergamo, M.; Bordignon, E.; Pelizzi, G. Mono- and Bis(hydrazine) Complexes of Osmium(II): Synthesis, Reactions, and X-ray Crystal Structure of the $[Os(NH_2NH_2)_2\{P(OEt)_3\}_4](BPh_4)_2$ Derivative. *Inorg. Chem.* **1998**, *37*, 479−489. (b) Albertin, G.; Antoniutti, S.; Bordignon, E.; Pattaro, S. Synthesis, Characterisation and Reactivity of Hydrazine Complexes of Iron(II). *J. Chem. Soc., Dalton Trans.* **1997**, 4445−4454. (c) Albertin, G.; Antoniutti, S.; Bacchi, A.; Bordignon, E.; Dolcetti, P. M.; Pelizzi, G. Preparation of mono- and bis-(hydrazine) complexes of ruthenium-(II). *J. Chem. Soc., Dalton Trans.* **1997**, 4435−4444. (d) Albertin, G.; Antoniutti, S.; Busato, C.; Castro, J.; Garcia-Fontan, S. Preparation and reactivity of penta- and tetracoordinate platinum(II) hydride complexes with $P(OEt)_3$ and $PPh(OEt)_2$ phosphite ligands. *Dalton Trans.* **2005**, 2641−2649. (e) Crossland, J. L.; Zakharov, L. N.; Tyler, D. R. Synthesis and Characterization of an Iron(II) η^2-Hydrazine Complex. *Inorg. Chem.* **2007**, *46*, 10476−10478. (f) Field, L. D.; Li, H. L.; Dalgarno, S. J. Side-on Bound Diazene and Hydrazine Complexes of Ruthenium. *Inorg. Chem.* **2010**, *49*, 6214−6221. (g) Field, L. D.; Li, H. L.; Dalgarno, S. J.; Jensen, P.; McIntosh, R. D. Synthesis and Characterization of Iron(II) and Ruthenium(II) Hydrido Hydrazine Complexes. *Inorg. Chem.* **2011**, *50*, 5468−5476. (h) Saouma, C. T.; Lu, C. C.; Peters, J. C. Mononuclear Five- and Six-Coordinate Iron Hydrazido and Hydrazine species. *Inorg. Chem.* **2012**, *51*, 10043−

DOI: 10.1021/acs.inorgchem.6b01550
Inorg. Chem. 2016, 55, 10284−10293

10054. (i) Field, L. D.; Li, H. L.; Dalgarno, S. J.; McIntosh, R. D. Base-Induced Dehydrogenation of Ruthenium Hydrazine Complexes. *Inorg. Chem.* **2013**, *52*, 1570−1583.
(8) (a) Xu, W.; Lough, A. J.; Morris, R. H. Competition between NH···HIr Intramolecular Proton−Hydride Interactions and NH···FBF_3- or NH···O Intermolecular Hydrogen Bonds Involving $[IrH(2\text{-thiazolidinethione})_4(PCy_3)](BF_4)_2$ and Related Complexes. *Inorg. Chem.* **1996**, *35*, 1549−1555. (b) Xu, W.; Lough, A. J.; Morris, R. H. Weak M-H—H-C Interactions Observed in Ruthenium and Iridium Complexes Containing Hydride, Amine, and Bulky Phosphine Ligands. *Can. J. Chem.* **1997**, *75*, 475−482. (c) Albertin, G.; Antoniutti, S.; Bordignon, E.; Menegazzo, F. Synthesis and Reactivity of Hydrazine Complexes of Iridium(III). *J. Chem. Soc., Dalton Trans.* **2000**, 1181−1189. (d) Matsukawa, S.; Kuwata, S.; Ishii, Y.; Hidai, M. Coordination Behaviour of (Diaryl Disulfide)-Bridged Dinuclear Thiairidaindan Cores: Ligand Substitution by Isocyanides, CO, Hydrazines and Hydroxylamine, and Related Reactions. *J. Chem. Soc., Dalton Trans.* **2002**, 2737−2746. (e) Seino, H.; Saito, A.; Kajitani, H.; Mizobe, Y. Properties and Reactivities of the Hydrido Ligands in Iridium Sulfido Clusters Relevant to Activation and Production of H_2. *Organometallics* **2008**, *27*, 1275−1289.
(9) (a) Hoover, J. M.; Freudenthal, J.; Michael, F. E.; Mayer, J. M. Reactivity of Low-Valent Iridium, Rhodium, and Platinum Complexes with Di- and Tetrasubstituted Hydrazines. *Organometallics* **2008**, *27*, 2238−2245. (b) Huang, Z.; Zhou, J.; Hartwig, J. F. N-H Activation of Hydrazines by Iridium(I). Double N-H Activation To Form Iridium Aminonitrene Complexes. *J. Am. Chem. Soc.* **2010**, *132*, 11458−11460.
(10) Lukehart, C.; Zeile, J. V. Reactions of Coordinated Molecules. XI. The Reaction of the Rhenium Tetracarbonyl Metallo-Acetylacetone Complex with Hydrazines. *J. Organomet. Chem.* **1977**, *140*, 309−316.
(11) Ciganda, R.; Garralda, M. A.; Ibarlucea, L.; Mendicute-Fierro, C.; Torralba, M. C.; Torres, M. R. Reactions of Hydridoirida-β-diketones with Amines or with 2-Aminopyridines. Formation of Hydridoirida-β-ketoimines, PCN Terdentate Ligands and Acyl Decarbonylation. *Inorg. Chem.* **2012**, *51*, 1760−1768.
(12) (a) Ciganda, R.; Garralda, M. A.; Ibarlucea, L.; Pinilla, E.; Torres, M. R. A Hydridoirida-β-diketone as Efficient and Robust Homogeneous Catalyst for the Hydrolysis of Ammonia-Borane or Amine-Borane Adducts in Air to Produce Hydrogen. *Dalton Trans.* **2010**, *39*, 7226−7229. (b) Garralda, M. A.; Mendicute-Fierro, C.; Rodríguez-Diéguez, A.; Seco, J. M.; Ubide, C.; Zumeta, I. Efficient Hydridoirida-β-diketone-Catalyzed Hydrolysis of Ammonia or Amine Boranes for Hydrogen Generation in Air. *Dalton Trans.* **2013**, *42*, 11652−11660. (c) Zumeta, I.; Mendicute-Fierro, C.; Rodríguez-Diéguez, A.; Seco, J. M.; Garralda, M. A. Acyliridium(III) Complexes with New PCN Terdentate Ligands Including Imino- or Iminium-acyl Moieties or Formation of Hydrido from Hydroxyl. *Eur. J. Inorg. Chem.* **2016**, *2016*, 1790−1797.
(13) (a) Clapham, S. E.; Hadzovic, A.; Morris, R. H. Mechanisms of the H_2-Hydrogenation and Transfer Hydrogenation of Polar Bonds Catalyzed by Ruthenium Hydride Complexes. *Coord. Chem. Rev.* **2004**, *248*, 2201−2237. (b) Gladiali, S.; Alberico, E. Asymmetric Transfer Hydrogenation: Chiral Ligands and Applications. *Chem. Soc. Rev.* **2006**, *35*, 226−236. (c) Samec, J. S. M.; Bäckvall, J. E.; Andersson, P. G.; Brandt, P. Mechanistic Aspects of Transition Metal-Catalyzed Hydrogen Transfer Reactions. *Chem. Soc. Rev.* **2006**, *35*, 237−248.
(14) Acha, F.; Ciganda, R.; Garralda, M. A.; Hernández, R.; Ibarlucea, L.; Pinilla, E.; Torres, M. R. Reactivity of Hydridoirida-β-diketones with Bases: The Selective Formation of New Di-μ-acyl-μ-hydridodiiridium(III) or Dihydridoirida-β-diketone Complexes and of Heterometallic Ir(III)/Rh(I) Derivatives. *Dalton Trans.* **2008**, 4602−4611.
(15) (a) Aguilar-Parrilla, F.; Scherer, G.; Limbach, H. H.; Foces-Foces, M. C.; Hernández-Cano, F.; Smith, J. A. S.; Toiron, C.; Elguero, J. Observation of a Series of Degenerate Cyclic Double, Triple, and Quadruple Proton Transfers in Solid Pyrazoles. *J. Am. Chem. Soc.* **1992**, *114*, 9657−9659. (b) de Paz, J. L. G.; Elguero, J.; Foces-Foces, C.; Llamas-Saiz, A. L.; Aguilar-Parrilla, F.; Klein, O.; Limbach, H. H. Theoretical Study of the Structure and Tautomerism of **N**1-Unsubstituted Pyrazoles in the Solid State. *J. Chem. Soc., Perkin Trans. 2* **1997**, *2*, 101−109. (c) Elguero, J.; Marzin, C.; Katrizky, A. R.; Linda, P. *The Tautomerism of Heterocycles*; Academic Press: New York, 1976; p 266. (d) Alkorta, I.; Rozas, I.; Elguero, J. A Computational Approach to Intermolecular Proton Transfer in the Solid State: Assistance by Proton Acceptor Molecules. *J. Chem. Soc., Perkin Trans. 2* **1998**, 2671−2676. (e) Chermahini, A. N.; Teimouri, A. Theoretical Studies on Proton Transfer Reaction of 3(5)-Substituted Pyrazoles. *J. Chem. Sci.* **2014**, *126*, 273−281.
(16) Chermahini, A. N.; Teimouri, A.; Beni, A. S.; Dordahan, F. Theoretical Studies on the Effect of Substituent in the Proton Transfer Reaction of 4-Substituted Pyrazoles. *Comput. Theor. Chem.* **2013**, *1008*, 67−73.
(17) Garralda, M. A.; Hernández, R.; Ibarlucea, L.; Pinilla, E.; Torres, M. R. Synthesis and Characterization of Hydridoirida-β-diketones Formed by the Reaction of $\{[Ir(Cod)Cl\}_2]$ (Cod = 1,5-cyclooctadiene) with o-(Diphenylphosphino)benzaldehdyde. *Organometallics* **2003**, *22*, 3600−3603.
(18) (a) Maslen, E. N.; Cannon, J. R.; White, A. H.; Willis, A. C. Crystal Structure of 3-Methyl-5-phenylpyrazole. *J. Chem. Soc., Perkin Trans. 2* **1974**, 1298−1301. (b) Aguilar-Parrilla, F.; Cativiela, C.; Diaz de Villegas, M. D.; Elguero, J.; Foces-Foces, C.; García-Laureiro, J. I.; Hernández-Cano, F.; Limbach, H. H.; Smith, J. A. S.; Toiron, C. The Tautomerism of 3(5)-Phenylpyrazoles: An Experimental (^1H, ^{13}C, ^{15}N NMR and X-ray Crystallography) Study. *J. Chem. Soc., Perkin Trans. 2* **1992**, 1737−1742. (c) Raptis, R. G.; Staples, R. J.; King, C.; Fackler, J. P., Jr. Structure of $[3,5\text{-}(C_6H_5)_2C_3H_2N_2]_4$. A 3,5-Diphenylpyrazole Tetramer Linked by Hydrogen Bonds. *Acta Crystallogr., Sect. C: Cryst. Struct. Commun.* **1993**, *49*, 1716−1719.
(19) Dougan, S. J.; Melchart, M.; Habtemariam, A.; Parsons, S.; Sadler, P. J. Phenylazo-pyridine and Phenylazo-pyrazole Chlorido Ruthenium(II) Arene Complexes: Arene Loss, Aquation, and Cancer Cell Cytotoxicity. *Inorg. Chem.* **2006**, *45*, 10882−10894.
(20) (a) Wright, L. Metallabenzenes and Metallabenzenoids. *J. Dalton Trans.* **2006**, 1821−1827. (b) Landorf, C. W.; Haley, M. M. Recent Advances in Metallabenzene Chemistry. *Angew. Chem., Int. Ed.* **2006**, *45*, 3914−3936. (c) Bleeke, J. R. Aromatic Iridacycles. *Acc. Chem. Res.* **2007**, *40*, 1035−1047. (d) Paneque, M.; Poveda, M. L.; Rendón, N. Synthesis and Reactivity of Iridacycles Containing the $Tp^{Me2}Ir$ Moiety. *Eur. J. Inorg. Chem.* **2011**, *2011*, 19−33. (e) Cao, X. Y.; Zhao, Q.; Lin, Z.; Xia, H. The Chemistry of Aromatic Osmacycles. *Acc. Chem. Res.* **2014**, *47*, 341−354. (f) Frogley, B. J.; Wright, L. J. Fused-ring Metallabenzenes. *Coord. Chem. Rev.* **2014**, *270*−*271*, 151−166.
(21) Garrou, P. E. DELTA.R-ring contributions to phosphorus-31 NMR parameters of transition-metal-phosphorus chelate complexes. *Chem. Rev.* **1981**, *81*, 229−266.
(22) Albertin, G.; Antoniutti, S.; Caia, A.; Castro, J. Preparation and Reactivity towards Hydrazines of Bis(cyanamide) and Bis(cyanoguanidine) Complexes of the iron triad. *Dalton Trans.* **2014**, *43*, 7314−7323.
(23) (a) Tillack, A.; Rudloff, I.; Beller, M. Catalytic Amination of Aldehydes to Amides. *Eur. J. Org. Chem.* **2001**, *2001*, 523−528. (b) Zhang, L.; Su, S.; Wu, H.; Wang, S. Synthesis of Amides through the Cannizzaro-Type Reaction Catalyzed by Lanthanide Chlorides. *Tetrahedron* **2009**, *65*, 10022−10224. (c) Li, Y.; Jia, F.; Li, Z. Iron-Catalyzed Oxidative Amidation of Tertiary Amines with Aldehydes. *Chem. - Eur. J.* **2013**, *19*, 82−86. (d) Bathini, T.; Rawat, V. S.; Bojja, S. In Situ Protection and Deprotection of Amines for Iron Catalyzed Oxidative Amidation of Aldehydes. *Tetrahedron Lett.* **2015**, *56*, 5656−5660. (e) Legacy, C. J.; Wang, A.; O'Day, B. J.; Emmert, M. H. Iron-Catalyzed Cα-H Oxidation of Tertiary, Aliphatic Amines to Amides under Mild Conditions. *Angew. Chem., Int. Ed.* **2015**, *54*, 14907−14910.
(24) Steiner, T. The Hydrogen Bond in the Solid State. *Angew. Chem., Int. Ed.* **2002**, *41*, 48−76.

DOI: 10.1021/acs.inorgchem.6b01550
Inorg. Chem. 2016, 55, 10284−10293

(25) NMR data for **8**: ^{1}H NMR ($CDCl_3$): δ 14.51 (s, 1H, N···H···O); −20.37 (t, 1H, ^{2}J(P,H) = 14.0 Hz, IrH). ^{31}P{^{1}H} NMR ($CDCl_3$): δ 31.1 (s); 15.5 (s).
(26) (a) Ackermann, M. N.; Hardy, L. C.; Xiao, Y. Z.; Dobmeyer, D. J.; Dunal, J. A.; Felz, K.; Sedman, S. A.; Alperovitz, K. F. Tungsten and Chromium Pentacarbonyl Complexes of Unsymmetric Dialkylhydrazines (RNHNHR′) and cis- and trans-Dialkyldiazenes (RN:NR′). *Organometallics* **1986**, *5*, 966−972. (b) Albertin, G.; Antoniutti, S.; Bonaldo, L.; Botter, A.; Castro, J. Azo Complexes of Osmium(II): Preparation and Reactivity of Organic Azide and Hydrazine Derivatives. *Inorg. Chem.* **2013**, *52*, 2870−2879. (c) Köthe, C.; Metzinger, R.; Herwig, C.; Limberg, C. Azo Complexes of Osmium-(II): Preparation and Reactivity of Organic Azide and Hydrazine Derivatives. *Inorg. Chem.* **2012**, *51*, 9740−9747.
(27) *APEX2*, version 1.08, *SAINT*, version 7.03, *SADABS*, version 2.11, and *SHELXTL*, version 6.12; Bruker Advanced X-ray Solutions: Madison, WI, 2004.
(28) Sheldrick, G. *SADABS: Program for Empirical Absorption Correction of Area Detector Data*; University of Göttingen: Göttingen, Germany, 1996.
(29) Altomare, A.; Burla, M. C.; Camalli, M.; Cascarano, G. L.; Giacovazzo, C.; Guagliardi, A.; Moliterni, A. G. G.; Polidori, G.; Spagna, R. SIR97: a New Tool for Crystal Structure Determination and Refinement. *J. Appl. Crystallogr.* **1999**, *32*, 115−119.
(30) (a) Sheldrick, G. M. *Program for Crystal Structure Refinement*; University of Göttingen, Göttingen, Germany, 2014. (b) Farrugia, L. J. WinGX Suite for Small-Molecule Single-Crystal Crystallography. *J. Appl. Crystallogr.* **1999**, *32*, 837−838.
(31) Spek, A. L. Single-Crystal Structure Validation with the Program PLATON. *J. Appl. Crystallogr.* **2003**, *36*, 7−13.
(32) Frisch, M. J.; Trucks, G. W.; Schlegel, H. B.; Scuseria, G. E.; Robb, M. A.; Cheeseman, J. R.; Scalmani, G.; Barone, V.; Mennucci, B.; Petersson, G. A.; Nakatsuji, H.; Caricato, M.; Li, X.; Hratchian, H. P.; Izmaylov, A. F.; Bloino, J.; Zheng, G.; Sonnenberg, J. L.; Hada, M.; Ehara, M.; Toyota, K.; Fukuda, R.; Hasegawa, J.; Ishida, M.; Nakajima, T.; Honda, Y.; Kitao, O.; Nakai, H.; Vreven, T.; Montgomery, J. A., Jr.; Peralta, J. E.; Ogliaro, F.; Bearpark, M.; Heyd, J. J.; Brothers, E.; Kudin, K. N.; Staroverov, V. N.; Kobayashi, R.; Normand, J.; Raghavachari, K.; Rendell, A.; Burant, J. C.; Iyengar, S. S.; Tomasi, J.; Cossi, M.; Rega, N.; Millam, J. M.; Klene, M.; Knox, J. E.; Cross, J. B.; Bakken, V.; Adamo, C.; Jaramillo, J.; Gomperts, R.; Stratmann, R. E.; Yazyev, O.; Austin, A. J.; Cammi, R.; Pomelli, C.; Ochterski, J. W.; Martin, R. L.; Morokuma, K.; Zakrzewski, V. G.; Voth, G. A.; Salvador, P.; Dannenberg, J. J.; Dapprich, S.; Daniels, A. D.; Farkas, Ö.; Foresman, J. B.; Ortiz, J. V.; Cioslowski, J.; Fox, D. J. *Gaussian 09*, revision D.01; Gaussian, Inc.: Wallingford, CT, 2009.
(33) (a) Becke, A. D. Density-Functional Thermochemistry. III. The Role of Exact Exchange. *J. Chem. Phys.* **1993**, *98*, 5648−5652. (b) Lee, C.; Yang, W.; Parr, R. G. Development of the Colle-Salvetti Correlation-Energy Formula into a Functional of the Electron Density. *Phys. Rev. B: Condens. Matter Mater. Phys.* **1988**, *37*, 785−789. (c) Vosko, S. H.; Wilk, L.; Nusair, M. Accurate Spin-Dependent Electron Liquid Correlation Energies for Local Spin Density Calculations: a Critical Analysis. *Can. J. Phys.* **1980**, *58*, 1200−1211. (d) Stephens, P. J.; Devlin, F. J.; Chabalowski, C. F.; Frisch, M. J. Ab Initio Calculation of Vibrational Absorption and Circular Dichroism Spectra Using Density Functional Force. *J. Phys. Chem.* **1994**, *98*, 11623−11627.
(34) (a) Hay, P. J.; Wadt, W. R. Ab Initio Effective Core Potentials for Molecular Calculations. Potentials for the Transition Metal Atoms Sc to Hg. *J. Chem. Phys.* **1985**, *82*, 270−283. (b) Wadt, W. R.; Hay, P. Ab Initio Effective Core Potentials for Molecular Calculations. Potentials for Main Group Elements Na to Bi. *J. Chem. Phys.* **1985**, *82*, 284−298. (c) Hay, P. J.; Wadt, W. R. Ab Initio Effective Core Potentials for Molecular Calculations. Potentials for K to Au Including the Outermost Core Orbitals. *J. Chem. Phys.* **1985**, *82*, 299−310.
(35) (a) Tomasi, J.; Mennucci, B.; Cammi, R. Quantum Mechanical Continuum Solvation Models. *Chem. Rev.* **2005**, *105*, 2999−3093. (b) Cossi, M.; Barone, V.; Cammi, R.; Tomasi, J. Ab Initio Study of Solvated Molecules: A New Implementation of the Polarizable Continuum Model. *Chem. Phys. Lett.* **1996**, *255*, 327−335. (c) Tomasi, J.; Persico, M. Molecular Interactions in Solution: An Overview of Methods Based on Continuous Distributions of the Solvent. *Chem. Rev.* **1994**, *94*, 2027−2094.

DOI: 10.1021/acs.inorgchem.6b01550
Inorg. Chem. 2016, 55, 10284−10293